MHD Flows in the Lower Expansion Chamber of a Generic Outboard Blanket Segment for DEMO

Leo Bühler, Chiara Mistrangelo, and Christina Koehly

***Abstract*—The water-cooled lead lithium (WCLL) blanket has been chosen as the European reference concept for a DEMO reactor. In the proposed design, liquid metal velocities in the columnar-arranged breeder units (BUs) are very small. This weak purge flow is required to circulate lead lithium (PbLi) toward external ancillary facilities for purification and tritium extraction. When the electrically conducting PbLi moves through the strong plasma-confining magnetic field, magnetohydrodynamics (MHD) affects the flow distribution and creates an increased pressure drop compared to hydrodynamic conditions. Previous MHD analyses have been performed for a single column of breeder units, with focus on the pressure drop in the poloidal manifolds that distribute PbLi among BUs. Manifolds have been identified as key and possibly critical components for the performance of blanket modules, since the major fraction of pressure drop arises in these elements. Moreover, they determine the partitioning of the PbLi flow among breeding zones. While the International Thermonuclear Experimental Reactor (ITER) Test Blanket Module (TBM) is designed only with two columns of BUs, in a DEMO reactor design, the number of parallel poloidal feeding and draining manifolds is larger. As a consequence, liquid metal has to be distributed from a single supply line into those channels via complex 3D geometries. In the present design of a DEMO blanket outboard segment, this is achieved by a toroidal expansion chamber located in the lower part of the module. The present analysis considers the MHD flow in this chamber, which expands from a radial circular entrance pipe along the toroidal direction toward two circular holes in the back plate of the blanket. Through these openings, the liquid metal is then distributed into the poloidal manifolds. Pressure and electric potential distributions are calculated via an asymptotic numerical approach valid for intense magnetic fields when inertia effects are negligible. Pressure losses, which arise preferentially from 3D MHD effects in expansion and contraction regions, are quantified.**

***Index Terms*—Flow distribution, liquid metal blankets, magnetohydrodynamics (MHD), pressure drop.**

I. Introduction

LIQUID metal alloys such as lead lithium (PbLi) are promising candidates for breeder material and heat transfer fluids in future fusion reactors. The European reference concept for a DEMO liquid metal blanket is a water-cooled lead lithium (WCLL) blanket, where the heat is removed by a large number of water-cooled pipes and where liquid metal in the columnar-arranged breeder units (BUs) serves as a breeder material. For purification and tritium extraction, the liquid metal is circulated toward external ancillary facilities. The BUs are fed and drained by a system of multiple poloidal manifolds along the back supporting structure of blanket sectors. Several feeding and draining manifolds are hydraulically connected to distributing and collecting chambers at the bottom and near the top of the module, respectively. When the electrically conducting PbLi moves through the plasma-confining magnetic field, magnetohydrodynamics (MHD) affects the flow distribution and creates an increased pressure drop compared to hydrodynamic conditions.

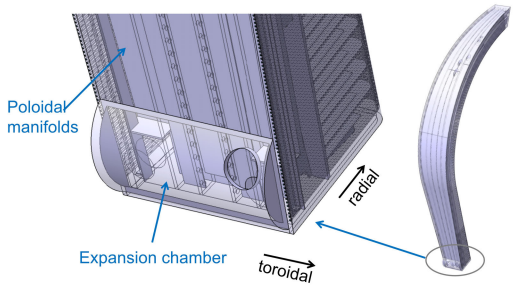

Fig. 1. Geometry of a lateral outboard module (right) and an enlarged view of the expansion chamber (left).

Previous liquid metal MHD analyses have been performed for a single column of BUs, as present, for instance, in the Test Blanket Module (TBM) for the International Thermonuclear Experimental Reactor (ITER). They focused on pressure drop in manifolds and flow distribution among BUs. Manifolds have been identified as key components for the performance of blanket modules, since the major fraction of pressure drop arises in these elements [1]. Their design eventually determines the liquid metal flow partitioning in BUs [2], [3] [4], [5]. While the ITER TBM consists only of two columns of BUs, in a DEMO blanket design, the number of parallel poloidal manifolds is much larger. Those channels have to be fed with liquid metal distributed from a single supply line. This is achieved in the current design of an outboard blanket segment by an expansion chamber in the lower part of the module. A corresponding collection chamber must be present near the upper end of the module.

Received 5 August 2025; accepted 26 February 2026. This work was supported by EUROfusion Consortium, through the European Union via Euratom Research and Training Program under Grant 101052200—EUROfusion. The review of this article was arranged by Senior Editor M. Kovari. *(Corresponding author: Leo Bühler.)*

The authors are with Karlsruhe Institute of Technology, 76021 Karlsruhe, Germany (e-mail: leo.buehler@kit.edu; chiara.mistrangelo@kit.edu; christina.koehly@kit.edu).

Color versions of one or more figures in this article are available at https://doi.org/10.1109/TPS.2026.3670923.

Digital Object Identifier 10.1109/TPS.2026.3670923

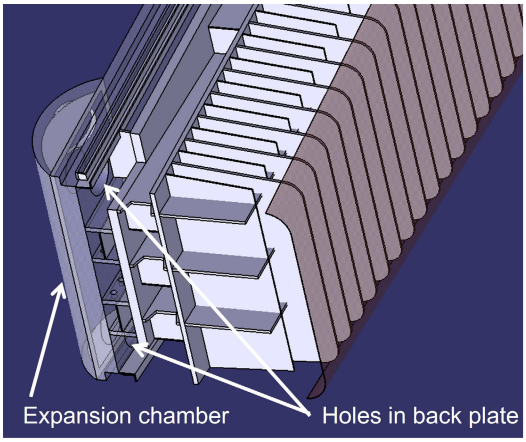

Fig. 2. Detailed view of the expansion chamber.

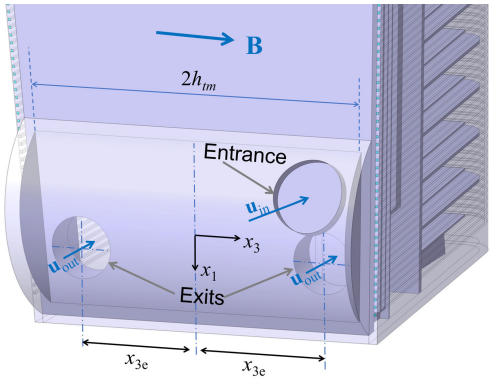

Fig. 3. Transparent view of the expansion chamber of a lateral outboard segment.

In the present work, we consider the MHD flow in a generic geometry related to a left outboard module of a WCLL blanket according to the current DEMO design. The lower part of the DEMO outboard module is shown in Figs. 1 and 2. The expansion chamber consists of a cylinder segment with a toroidal length $2h_{tm}$ (subscript tm denotes toroidal manifold) to which the liquid metal is supplied via an entrance pipe (see Fig. 3). The factor 2 in the definition of the length scale results from the fact that in MHD simulations, the half characteristic size measured along magnetic field lines, the so-called Hartmann length, plays an important role for the definition of the dimensionless parameters (2). The figures display the expansion volume of the toroidal manifold with the entrance opening to which the inlet pipe (not displayed) will be connected. In the chamber, the flow expands in toroidal direction toward two circular holes in the thick back plate through which the liquid metal is distributed into the poloidal manifolds.

From the DEMO design, we derive a model geometry, the topology of which is displayed in Fig 4. It consists of an inlet pipe with radius r_i through which the liquid metal enters the toroidal expansion chamber. While in the original design, the entrance pipe has some inclination with respect to the x_2 coordinate (as indicated in gray), for the present analysis, we chose for simplicity the pipe axis along x_2. This should not

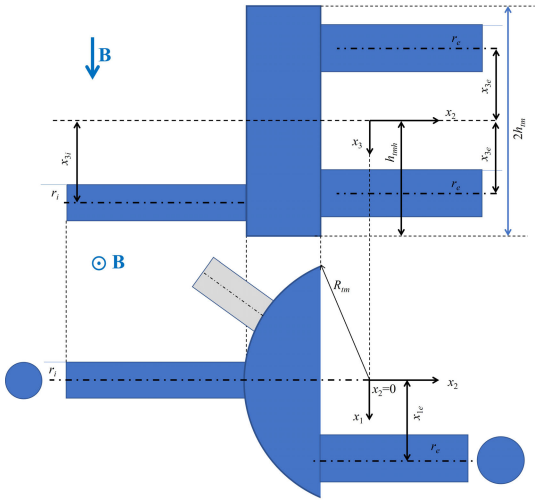

Fig. 4. Sketch of a model geometry (not to scale) showing the topology with an inlet pipe, a sector of a circular chamber forming the expansion volume that feeds two exit pipes. While in the design, the inlet pipe has some inclination with respect to the x_2 axis (see gray part) in the modeled geometry, we assume the inlet pipe being aligned with x_2 for simplicity.

impact much the results for pressure drop and flow distribution since the major 3D element, namely the expansion of the flow from the pipe into the larger chamber, is properly modeled. The latter one is formed by a sector of a circular cylinder of radius R_{tm}. Its half-length h_{tm} is measured along the toroidal direction x_3. The fluid leaves the chamber through two circular holes in the back plate with radius r_e, whose axes (or centers) are located at a distance x_{3e} from the "symmetry plane" of the chamber. For grid generation, the coordinate system used is centered on the axis of the toroidal chamber.

II. Mathematical Model

A. Governing Equations

We consider the incompressible flow of PbLi in a strong magnetic field. The flow is described by a balance of momentum in which the inertia force balances pressure, viscous, and electromagnetic Lorentz forces. In nondimensional notation, we have

$$\frac{1}{N}\left(\frac{\partial \mathbf{u}}{\partial t} + (\mathbf{u}\cdot\nabla)\,\mathbf{u}\right) = -\nabla p + \frac{1}{Ha^2}\nabla^2\mathbf{u} + \mathbf{j}\times\mathbf{B}. \quad (1)$$

The current density $\mathbf{j}$ that determines the strength of the Lorentz force $\mathbf{j} \times \mathbf{B}$ results from Ohm's law

$$\mathbf{j} = -\nabla\phi + \mathbf{u}\times\mathbf{B}.$$

Currents are driven by the gradient of electric potential ϕ and a flow-induced electric field $\mathbf{u} \times \mathbf{B}$. The flow is assumed incompressible with $\nabla\cdot\mathbf{u} = 0$ and charge conservation requires continuity of current density, $\nabla\cdot\mathbf{j} = 0$. In the equations above, $\mathbf{u}, \mathbf{B}, \mathbf{j}$, p, and ϕ denote fluid velocity, magnetic field, current density, pressure, and electric potential, scaled by the reference quantities u_0, B_0, $j_0 = \sigma u_0 B_0$, $p_0 = \sigma u_0 B_0^2 L$ and $\phi_0 = u_0 B_0 L$. The characteristic velocity u_0 is the half of the average velocity in the entrance pipe (because the flow is distributed in the chamber to two individual streams for each exit opening), B_0

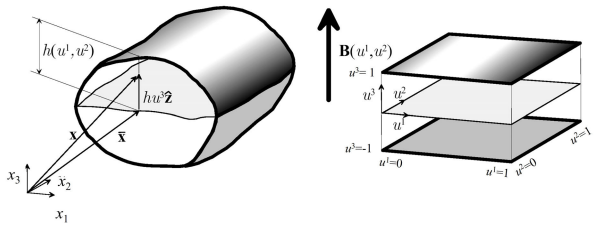

Fig. 5. Definition of a transformation that maps the physical domain (x_1, x_2, x_3) to a standard volume (u^1, u^2, u^3) on the surface of which (at $u^3 = \pm 1$) potential and pressure are determined [8], [10].

is the magnitude of the applied toroidal magnetic field, and $L = r_i$ is the typical length scale of the problem, chosen here as the inner radius of the entrance pipe.

With length scale L, mass density ρ, kinematic viscosity ν, and electric conductivity σ [6], the nondimensional parameters governing the flow, i.e., the interaction parameter N and the Hartmann number Ha, are defined as

$$N = \frac{\sigma L B^2}{\rho u_0} \text{and } Ha = LB\sqrt{\frac{\sigma}{\rho\nu}}. \tag{2}$$

In MHD flows, the parameters N and the square of the Hartmann number Ha^2 quantify the ratios of electromagnetic forces to inertia and viscous forces, respectively. The conductance of the solid walls of thickness t_w with conductivity σ_w compared to the conductance of the fluid region is quantified by the wall conductance parameter $c = t_w\sigma_w/L\sigma$, which is used in the global balance of wall currents in form of the thin-wall condition [7]

$$\mathbf{j}\cdot\mathbf{n} = \nabla_t\,(c\,\nabla_t\phi)$$

where ∇_t denotes the wall-tangential components of the gradient operator.

For strong magnetic fields, as in a fusion reactor, both parameters N and Ha are very large. The magnetic field is unaffected by the flow and given by the externally applied toroidal field $\mathbf{B} = B\hat{\mathbf{x}}_3$. For strong magnetic fields, as $N \to \infty$, $Ha \gg 1$, the electromagnetic force is dominant and balanced in the core by the pressure gradient

$$\nabla p = \mathbf{j}\times\mathbf{B}$$

i.e., the core flow is inviscid and inertialess. Viscous effects are present only in thin boundary layers, where they are taken into account by a viscous correction. The equations allow for an analytical integration along magnetic field lines using values of variables at the wall as integration functions, depending on their position at the fluid–wall interface. Once the results on the wall are determined by numerical means using boundary-fitted coordinates, it is possible to reconstruct the full 3D flow field. Details of the asymptotic analysis based on tensor formulation are described in [8].

B. Boundary-Fitted Grid

For applications of the asymptotic method to sudden expansions with walls aligned with the magnetic field (here the cylindrical expansion volume) or for abrupt contractions (holes

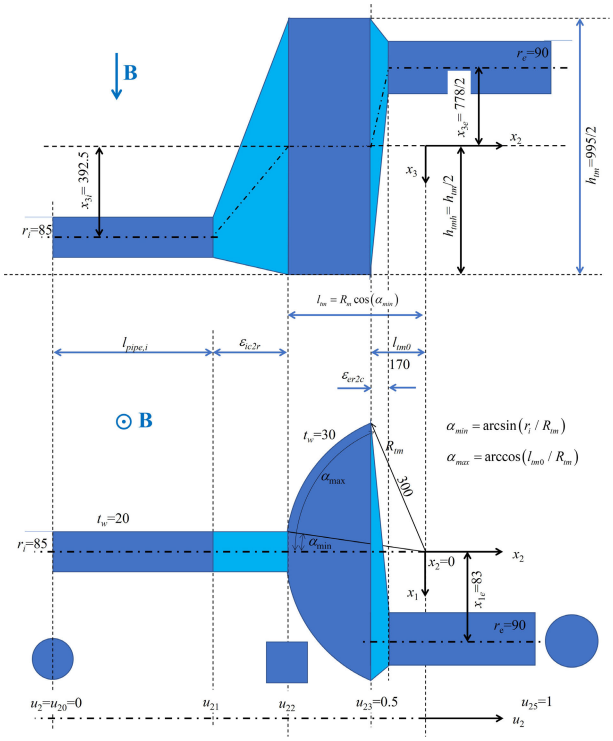

Fig. 6. Sketch of a model geometry (not to scale) showing the grid topology with an inlet pipe, with transition from circular to rectangular shape along a length ϵ_{ic2r} at the inlet pipe and a sector of a circular cylinder forming the expansion volume. A second transition region of length ϵ_{er2c} connects the rectangular back plate with the circular exit pipe. The transition regions ϵ are shown here enlarged for a better understanding of the grid topology. For numerical simulations, both values have been taken as small as 0.01 r_i.

on the back plate), those geometrical transitions are modeled as continuous variations from one cross section to the other one, along a short but finite length ϵ. In a systematic analysis for expanding flows with varying expansion length ϵ it has been demonstrated that results, and in particular those for Δp_{3D}, converge to correct finite values as $\epsilon \to 0$, i.e., to the results of a sudden expansion [9]. For the present simulations, we have chosen the nondimensional transition length as short as $\epsilon_{ic2r} = 0.01$ for the circular to rectangular transition at the inlet pipe and $\epsilon_{er2c} = 0.01$ for the transition from the rectangular back wall to the circular exit openings in that wall. For details on the grid topology, see Fig. 6. The figure defines the coordinates that are used to map the geometry described in Cartesian coordinates (x_1, x_2, x_3) to the standard volume $(0 < u^1 < 1, 0 < u^2 < 1, -1 < u^3 < 1)$ on the surface of which electric potential and pressure are calculated. For more details, see [8] or Fig. 5.

Since the method in its standard version can handle only *one* entrance and *one* exit, the problem is split into two subproblems, i.e., a *case 1* with a flow that feeds only one outlet pipe and another *case 2* with a flow that feeds the second outlet. The final solution is obtained as a superposition of both fundamental solutions. One has to admit that this procedure is not exact in a mathematical sense, but it seems appropriate for the determination of pressure drop in the considered geometry of an expansion chamber.

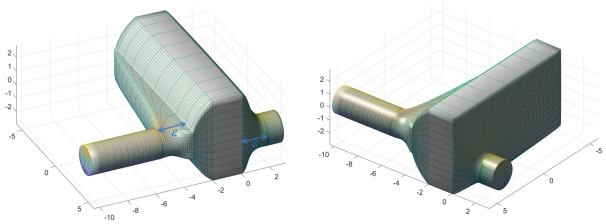

Fig. 7. View on a boundary-fitted grid with longer transition regions ϵ for better visualization of the grid topology.

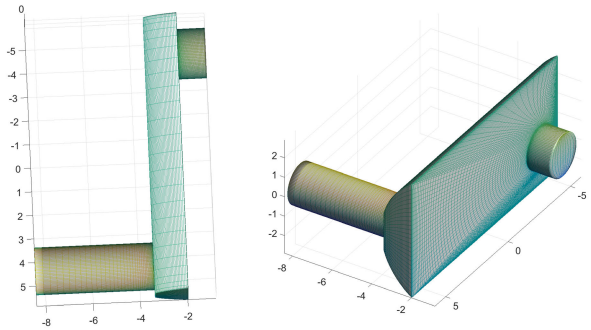

Fig. 8. View on the boundary-fitted grid used for the simulations of *case 1*.

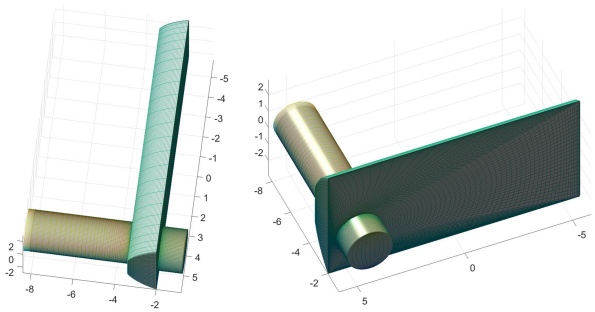

Fig. 9. View on the boundary-fitted grid used for the simulations of *case 2*.

TABLE I

PBLI PROPERTIES AT 300 °C ACCORDING TO [6]. THE ELECTRICAL CONDUCTIVITY OF EUROFER IS TAKEN FROM [11]

T	ρ	ν	σ	σ_w
$[^\circ\mathrm{C}]$	$[\mathrm{kg/m^3}]$	$[10^{-6}\mathrm{m^2/s}]$	$[10^6/\Omega\mathrm{m}]$	$[10^6/\Omega\mathrm{m}]$
300	9838	0.214	0.883	1.19

Fig. 7 shows the grid topology for an example with larger transition lengths ϵ with the purpose of explaining how the grid is composed. For the final calculations, ϵ has been chosen as small as $\epsilon = 0.01\, r_i$.

The grid on the fluid–wall interface, as used in the simulations of the flow in the expansion chamber, is shown in Figs. 8 and 9 for the two considered cases.

III. RESULTS

Simulations for MHD flows in the lower expansion chamber of a lateral outboard segment have been performed by applying the analysis outlined above. With operational parameters according to Table II and thermophysical properties of PbLi at 300 °C according to Table I [6], the Hartmann number defined in (2) becomes $Ha = 8512$. Each wall is considered with its individual wall conductance ratio c according to the local wall thickness.

TABLE II

TYPICAL DEMO PARAMETERS FOR THE FLOW IN THE LOWER EXPANSION CHAMBER OF THE LATERAL OUTBOARD SEGMENT

B	Q	$u_0 = \frac{1}{2}\frac{Q}{\rho\pi r_i^2}$	r_i	Ha	N
$[T]$	$[\mathrm{kg/s}]$	$[\mathrm{m/s}]$	$[\mathrm{m}]$		
4.89	14	0.0314	0.085	8512	5809

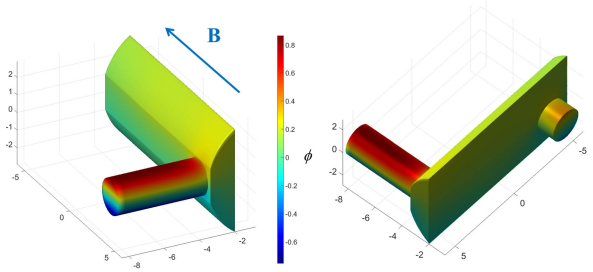

Fig. 10. MHD flow in the lower expansion chamber for $Ha = 8512$. Colored contours for nondimensional electric potential ϕ at the fluid–wall interface for *case 1*.

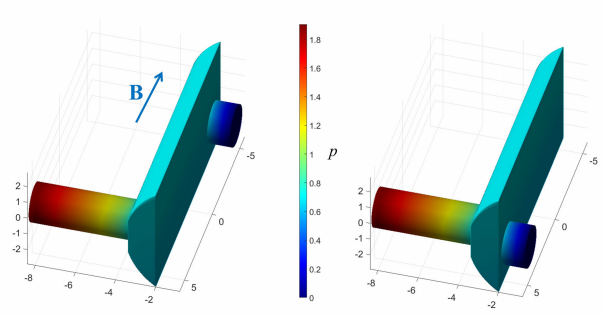

Fig. 11. MHD flow in the lower expansion chamber for $Ha = 8512$. Colored contours of nondimensional pressure at the fluid–wall interface for *case 1* (left) and *case 2* (right).

Results for electric potential ϕ plotted on the fluid–wall interface are shown for *case 1* in Fig. 10. We observe that the highest potential values occur at the entrance pipe, where the velocity is the largest. When the flow expands along the chamber, velocity and potential reduce significantly. Although velocity in the exit hole is of a similar order of magnitude as in the entrance pipe, the potential here is much smaller since currents find an efficient shortcut in the thick back plate.

Fig. 11 presents results for pressure, plotted on the fluid–wall interface for both *case 1* and *case 2*. Since pressure does not vary along magnetic field lines, the figures already give a good impression of the pressure distribution in the fluid.

More details about the distribution of nondimensional pressure can be seen from Fig. 12 (bottom), where pressure along the radial coordinate x_2 is displayed for *case 2*. It can be seen that the entrance pipe has been chosen long enough that fully established conditions with a uniform pressure gradient are established at the inlet. When approaching the expansion

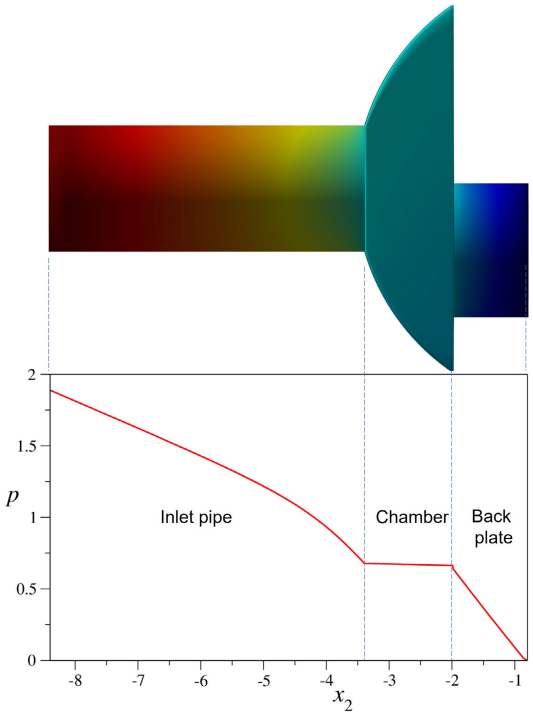

Fig. 12. MHD flow in the lower expansion chamber for Ha = 8512. Pressure distribution for *case 2*. Colored contours of pressure at the fluid–wall interface (top), pressure along the radial coordinate x_2 (bottom).

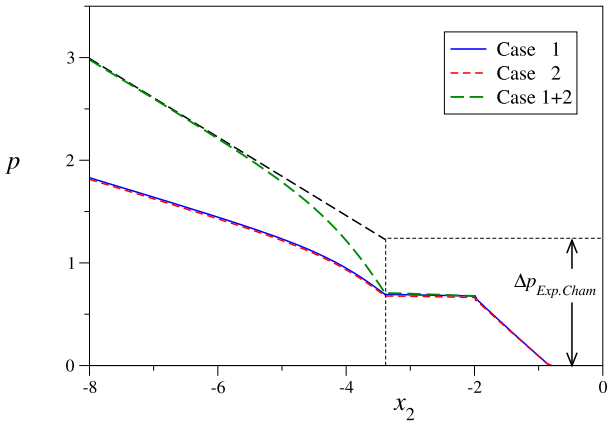

Fig. 13. MHD flow in the lower expansion chamber for Ha = 8512. Pressure distribution along the radial coordinate x_2 for *case 1* and *case 2* and for the combined case.

volume, the pressure drops more rapidly due to additional 3D currents and extra Lorentz forces. Inside the expansion chamber, the velocities are much smaller since the dimensions are larger. Therefore, the radial pressure decrease inside the chamber remains small. We also observe that a significant fraction of the pressure drop occurs when the fluid passes through the thick back plate. This is due to the fact that the thick wall provides a shortcut for induced currents, resulting in increased core current density and higher Lorentz forces in the fluid.

Results similar to those shown for *case 2* in Fig. 12 are also obtained for *case 1* and displayed in Fig. 13 (blue curve). It can be observed that both results almost coincide. A reason for that coincidence is that the major fractions of pressure drop occur along the inlet pipe and at the entrance to the expansion chamber, and when the flow leaves the chamber through the exit holes. Those contributions are almost the same for both cases. The flow across the expansion chamber also shows nearly the same variation since along magnetic field lines the pressure is constant and inertia effects are negligible. When we "assemble" the results for the combined flow in the complete geometry (see Fig. 4), then the flow in each exit pipe remains unaffected since the flow there is the same as for *case 1* and *case 2*. In the entrance pipe and the expansion chamber, the mass flow rate is given by the sum of the individual cases. Therefore, for pressure drop, we have contributions from both cases that sum up to the combined result shown as a green dashed line.

The focus of the present work is on the MHD flow in the expansion chamber. Results displayed in Fig. 13, however, consist of contributions from the circular entrance pipe flow and 3D effects when approaching the entrance to the expansion volume. In the following, we separate the effects of MHD pressure drop in the toroidal expansion chamber from those of the supplying lines. This is required since details of the entrance pipe (length, orientation, etc.) are yet to be defined in the design concept. For that purpose, we extrapolate the pressure variation along the entrance pipe toward the expansion chamber and identify the contribution $\Delta p_{ExpCham}$, which can be attributed to this part of the geometry. The present asymptotic analysis results in a nondimensional value

$$\Delta p_{ExpCham} = 1.23$$

from which the dimensional results follow as

$$\Delta p^*_{ExpCham} = u_0 \sigma L B^2 \Delta p_{ExpCham}.$$

The velocity scale introduced in Section II-A results from the mass flux Q of the lateral segment as

$$u_0 = \frac{1}{2}\frac{Q}{\rho \pi r_i^2}.$$

The thermophysical properties of PbLi are used according to [6] for a reference temperature of 300 °C (see Table I).

Operational parameters for the flow in the lower expansion chamber are listed in Table II.

According to the DEMO specifications, the total mass flow rate by one PbLi loop in a DEMO reactor is 169 kg/s. One loop supplies four sectors in the tokamak, each sector receiving 42.25 kg/s. A sector is formed by three subelements. Since so far no further details about flow partitioning between central and lateral elements are available, it is assumed that each receives the same amount of flow, i.e., 14 kg/s.

The magnitude of the toroidal magnetic field may vary along the outboard module in the range 3.35–5.21 T. For the present analysis, we use the value B_0 = 4.89 T at the radial position R_0 = 8.9 m [12]. As a final result, the dimensional pressure drop in the lower expansion chamber can be estimated as

$$\Delta p^*_{ExpCham} = u_0 \sigma L B^2 \Delta p_{ExpCham}$$
$$\Delta p^*_{ExpCham} = 0.0693\,\text{MPa}.$$

This value seems relatively small, but it covers only the additional contributions due to the 3D flow in one expansion chamber. A similar value is expected from 3D effects in the contraction chamber near the top of the module. The upper toroidal manifold was not yet present in the CAD design provided by EUROfusion.

IV. Conclusion

The present work considers the MHD flow in the lower expansion chamber, i.e., in the toroidal manifold of a lateral WCLL blanket module. The problem has been analyzed by applying an asymptotic analysis valid for large interaction parameters and high Hartmann numbers. The reduced equations are solved numerically on a boundary-fitted grid at the fluid–wall interface for two separate cases, and the results are later assembled for the final solution. As a major outcome of the analysis, we can estimate the pressure drop for the present problem being $\Delta p^*_{ExpCham} = 0.0693$ MPa, which seems acceptable. For the upper toroidal manifold, which should have a similar geometry, one should expect a value that is comparable to the present result.

The work discussed in this report relies on a couple of assumptions, such as inviscid and inertialess flows in the fluid cores, simplifications of the geometry, thin wall approximation, and the splitting of the problem into two separate cases. In order to verify if these assumptions are justified, it is planned to analyze the present problem by full numerical simulations. The latter will further allow us to complement the investigation by considering all magnetic field components, including a poloidal contribution. This is a topic of ongoing research.

Acknowledgment

This work has been carried out within the framework of the EUROfusion Consortium, funded by the European Union via the Euratom Research and Training Programme (Grant Agreement No 101052200 — EUROfusion). Views and opinions expressed are however those of the author(s) only and do not necessarily reflect those of the European Union or the European Commission. Neither the European Union nor the European Commission can be held responsible for them.

References

[1] L. Bühler, C. Mistrangelo, H.-J. Brinkmann, and C. Koehly, "Pressure distribution in MHD flows in an experimental test-section for a HCLL blanket," *Fusion Eng. Design*, vol. 127, pp. 168–172, Feb. 2018.

[2] C. Mistrangelo, L. Bühler, C. Koehly, and I. Ricapito, "Magnetohydrodynamic velocity and pressure drop in manifolds of a WCLL TBM," *Nucl. Fusion*, vol. 61, no. 9, Sep. 2021, Art. no. 096037.

[3] C. Courtessole, H.-J. Brinkmann, L. Bühler, and J. Roth, "Experimental investigation of MHD flows in a WCLL TBM mock-up," in *Proc. 15th Int. Symp. Fusion Nucl. Technol.*, Las Palmas de Gran Canaria, Spain, Sep. 2023, pp. 10–15.

[4] L. Bühler and C. Mistrangelo, "A simple MHD model for coupling poloidal manifolds to breeder units in liquid metal blankets," *Fusion Eng. Design*, vol. 191, Jun. 2023, Art. no. 113552.

[5] L. Bühler, C. Courtessole, C. Koehly, B. Lyu, and C. Mistrangelo, "Electric potential on a WCLL TBM mock-up in MHD experiments as indication for flow distribution in breeder units," *Presented at the 33rd Symp. Fusion Technol.*, vol. 212, Dublin, Ireland, Sep. 2025.

[6] D. Martelli, A. Venturini, and M. Utili, "Literature review of lead-lithium thermophysical properties," *Fusion Eng. Design*, vol. 138, pp. 183–195, Jan. 2019.

[7] J. S. Walker, "Magnetohydrodynamic flows in rectangular ducts with thin conducting walls," *J. de Mécanique*, vol. 20, no. 1, pp. 79–112, 1981.

[8] L. Bühler, "Magnetohydrodynamic flows in abitrary geometries in strong, nonuniform magnetic fields," *Fusion Technol.*, vol. 27, no. 1, pp. 3–24, 1995.

[9] L. Bühler, "A parametric study of 3D MHD flows in expansions of rectangular ducts," *Fusion Sci. Technol.*, vol. 52, no. 3, pp. 595–602, Oct. 2007.

[10] L. Bühler, "Liquid metal magnetohydrodynamics for fusion blankets," in *Magnetohydrodynamics Historical Evolution and Trends (Fluid Mechanics, and its Applications)*, S. Molokov, R. Moreau, and H. K. Moffatt, Eds., Dordrecht, The Netherlands: Springer, 2007, pp. 171–194.

[11] K. Mergia and N. Boukos, "Structural, thermal, electrical and magnetic properties of eurofer 97 steel," *J. Nucl. Mater.*, vol. 373, nos. 1–3, pp. 1–8, Feb. 2008.

[12] A. Tassone, S. Siriano, G. Caruso, M. Utili, and A. D. Nevo, "MHD pressure drop estimate for the WCLL in-magnet PbLi loop," *Fusion Eng. Design*, vol. 160, Nov. 2020, Art. no. 111830.

Leo Bühler received the Dr.-Ing. degree in fluid dynamics from Karlsruhe University, Karlsruhe, Germany, in 1992, and the Habilitation degree from Karlsruhe University in 2008.

He is currently a Professor with the Department for Thermal Energy Technology and Safety, KIT, Karlsruhe, and the Head of the MHD Research Group with MEKKA and MaPLE facilities. His research interests include any kind of MHD flow in generic and complex geometries, asymptotic analysis, code development, and validation through experiments.

Chiara Mistrangelo received the Ph.D. degree in fluid dynamics from Karlsruhe University, Karlsruhe, Germany, in 2005.

She is currently a Senior Researcher and a Lecturer with the Department for Thermal Energy Technology and Safety, KIT. Her current research interests include pressure-driven and buoyancy-driven convective MHD flows in complex geometries, code development, and validation through experiments and benchmark activities.

Christina Koehly received the B.S. degree in mechanical engineering from Baden-Württemberg Cooperative State University, Karlsruhe, Germany, in 2002, and the M.S. degree in mechanical engineering from Karlsruhe University of Applied Science, Karlsruhe, in 2006.

Since 2002, she has been with Karlsruhe Institute of Technology, Karlsruhe, working on several fusion and fission projects for future nuclear power plants with special interest in blanket engineering and mock-up design for MHD experiments.